

# Image segmentation techniques for cardiovascular biomedical applications

Alexander A. Danilov, Roman A. Pryamonosov, and Alexandra S. Yurova

Institute of Numerical Mathematics, Russian Academy of Sciences, Gubkina 8, Moscow, 119333, Russian Federation

Moscow Institute of Physics and Technology, Institutskiy 9, Dolgoprudny, 141701, Russian Federation

## Introduction

Methods and algorithms for patient-specific image segmentation and generation of discrete geometric models are presented for several cardiovascular medical applications. Hemodynamics modeling applications require individualized 1D or 3D regional network of blood vessels. Electrocardiography (ECG) modeling requires the segmentation of heart tissues and in some cases other soft tissues in the chest or in the whole body.

## Vascular network segmentation

Contrast enhanced Computed Tomography Angiography (ceCTA) DICOM images are used as input data. Our automatic vessel segmentation methodology for coronary and cerebral arteries was proposed in [1, 2, 3]. Essential steps of this method (Fig. 1): aorta segmentation, computation of Frangi vesselness values, searching branches of aortic arch and ostia points, removing segmentation errors near aorta boundary, skeletonization and 1D network reconstruction.

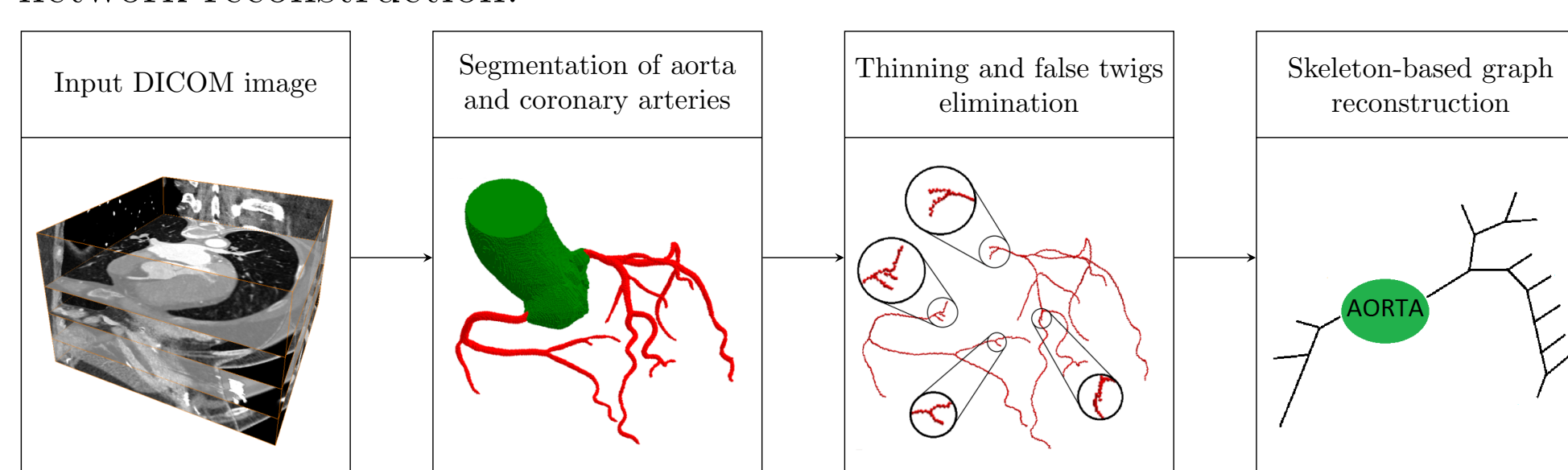


Figure 1: Flowchart for automatic reconstruction of coronary arteries 1D network.

Bone elimination is an essential step for cerebral artery segmentation due to vertebral arteries and cervical vertebrae proximity. The multiscale matched mask bone elimination algorithm [4] may be used if both CT and ceCTA datasets are available for the same patient. The isoperimetric distance trees [5] algorithm is used for aorta segmentation. The next step is computation of Frangi vesselness [6], which results in bigger values inside bright tubular structures. Vascular 1D computational network is reconstructed using skeletonization [7].

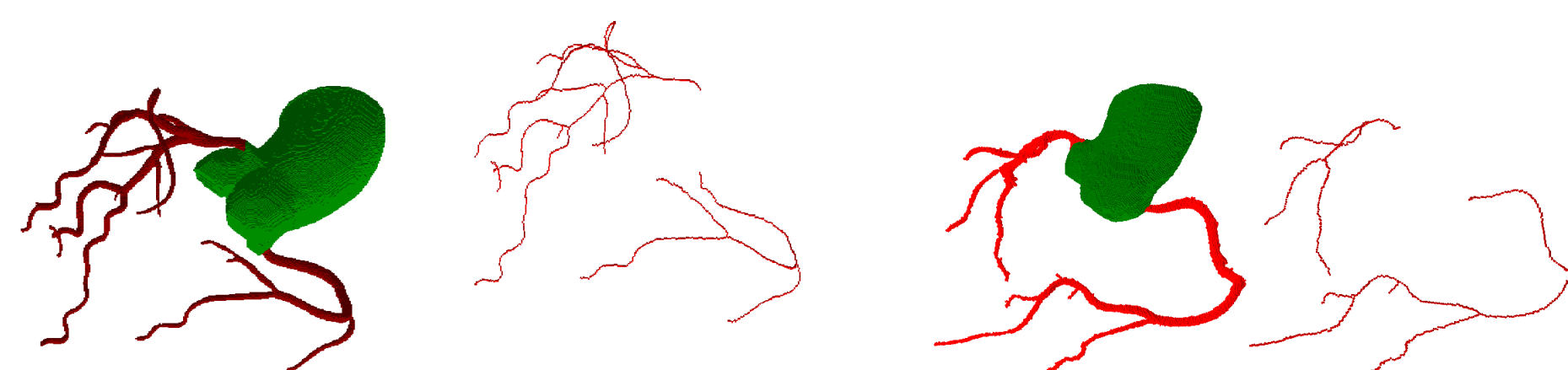


Figure 2: Segmentation and skeletonization for coronary datasets CD1 (left), CD2 (right).

In practice a skeleton may have several false twigs, usually near bifurcations and flattened vessels, which do not correspond to any actual vessel. Several post-processing stages are used to clean falsely detected parts of vascular network and improve segmentation quality.

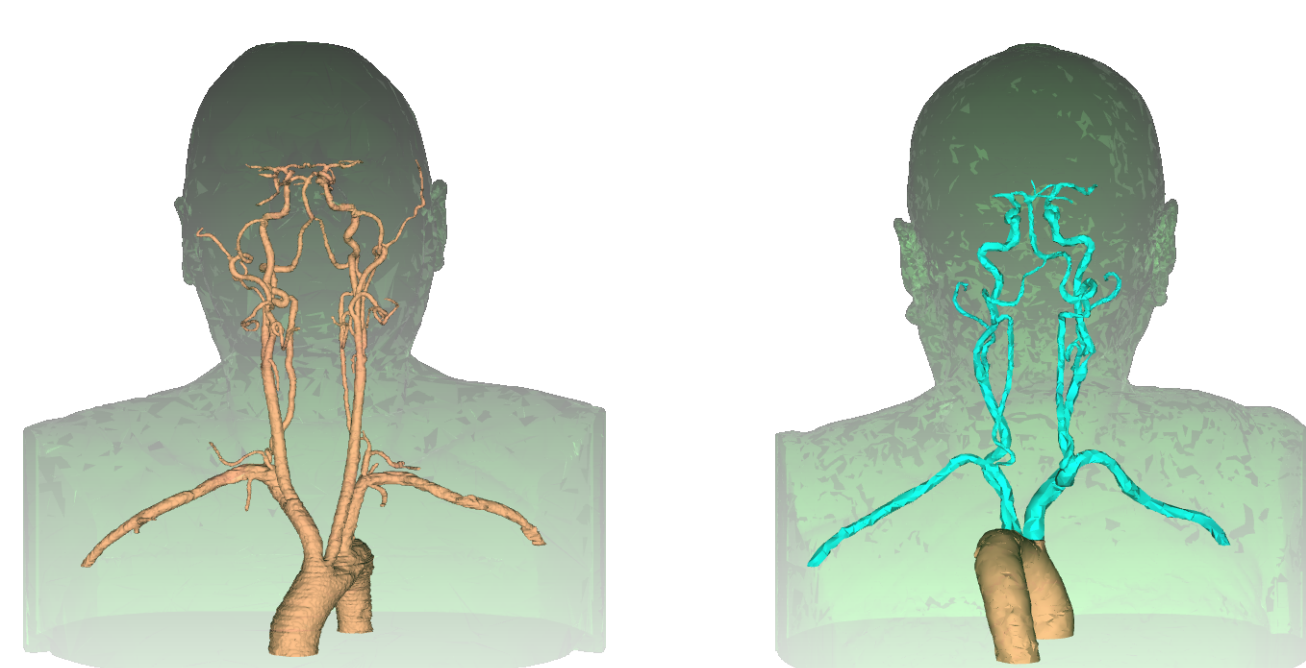


Figure 3: Cerebral arteries segmentation for datasets ND1 (left) and ND2 (right).

Results of automatic segmentation, skeletonization, and network reconstruction for two coronary datasets (CD1, CD2) and two cerebral datasets (ND1, ND2) are presented in Figs. 2–3. CPU times of specific segmentation and skeletonization stages are presented in Table 1.

Table 1: Dataset resolution and CPU times of segmentation stages.

Dataset	CD1	CD2
Resolution	512 × 512 × 248	512 × 512 × 211
Spacing	0.37 × 0.37 × 0.40 mm	0.46 × 0.46 × 0.48 mm
Aorta segmentation	5.80 s	5.19 s
Frangi filter	91.76 s	73.94 s
Dataset	ND1	ND2
Resolution	512 × 512 × 501	512 × 512 × 451
Spacing	0.76 × 0.76 × 0.80 mm	0.62 × 0.62 × 0.80 mm
Pulmonary removal	7.76 s	7.04 s
Aorta segmentation	16.61 s	15.33 s
Frangi vesselness	196.40 s	184.91 s
Aortic arch branches	7.61 s	6.67 s
Aorta border cleaning	7.39 s	6.76 s

## Dynamic left ventricle segmentation

We developed the technology for generation of a dynamic mesh for heart ventricles. The proposed pipeline was tested on the left ventricle using anonymized dynamic chest ceCT dataset of 100 images with 512 × 512 × 480 voxels and 0.625 × 0.625 × 0.25 mm resolution. We manually segmented several images: #0 – beginning of systole, #30 – end of systole, and #50 – middle of rapid inflow during diastole. Levelset method from ITK-SNAP package [8] was used for user-guided segmentation of four materials: left ventricle, left atrium, aorta, and right ventricle and atrium combined (Fig. 4-left).

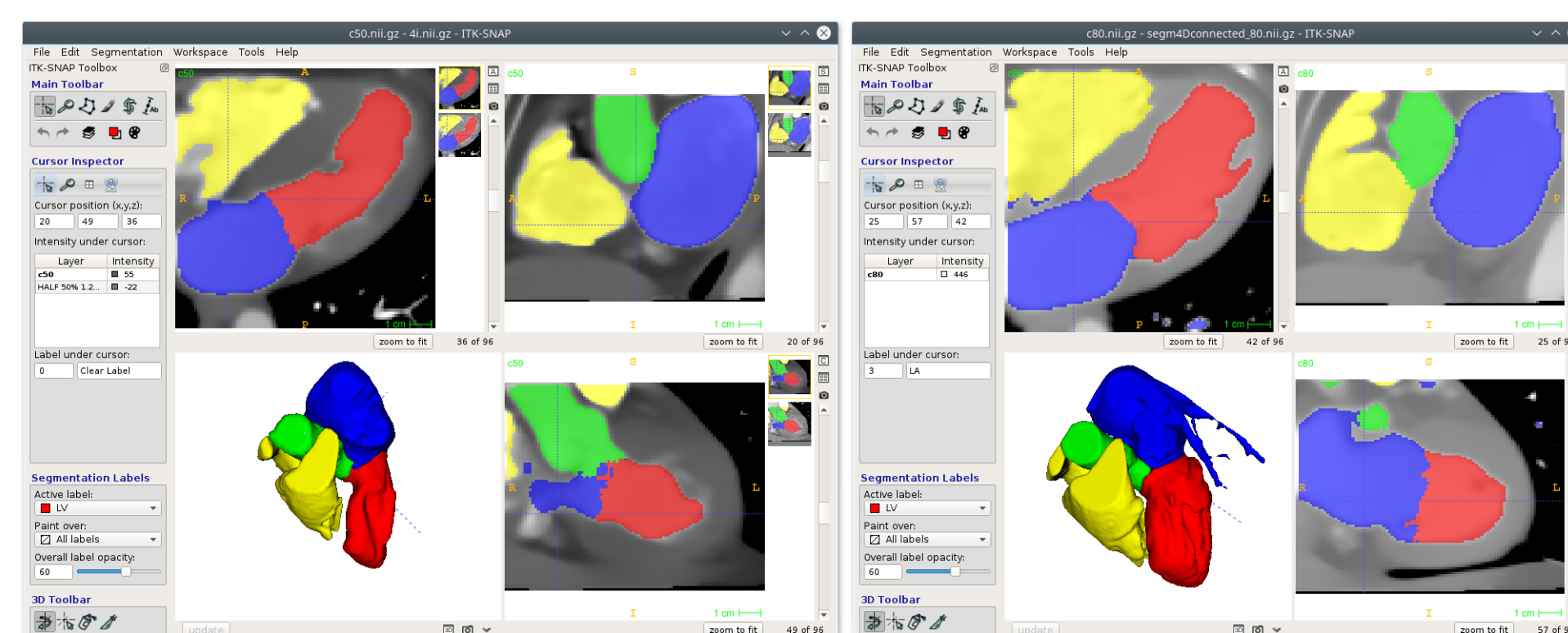


Figure 4: Segmentation of ceCT images: manual segmentation of image #50 (left), automatic segmentation of image #80 (right). Segmentation colors: left ventricle (red), left atrium (blue), aorta (green), right ventricle and atrium (yellow). Screenshots from ITK-SNAP software.

We trained random forest classifier on the manually segmented images and post-processed the result of classification using a combination of mathematical operations: dilation, erosion, and construction of connected regions (Fig. 4-right).



Figure 5: Dynamic left ventricle model. The video contains following stages: initial ceCT DICOM dataset, automatic segmentation, dynamic surface and volumes meshes, and computed velocity field.

The initial unstructured tetrahedral mesh is constructed for image #0 and then deformed by node movements for each subsequent image (Fig. 5). Boundary nodes are moved first simultaneously propagating and smoothing the surface mesh (Fig. 6-top). Internal nodes are shifted by simultaneous untangling and smoothing algorithm [9] (Fig. 6-bottom).

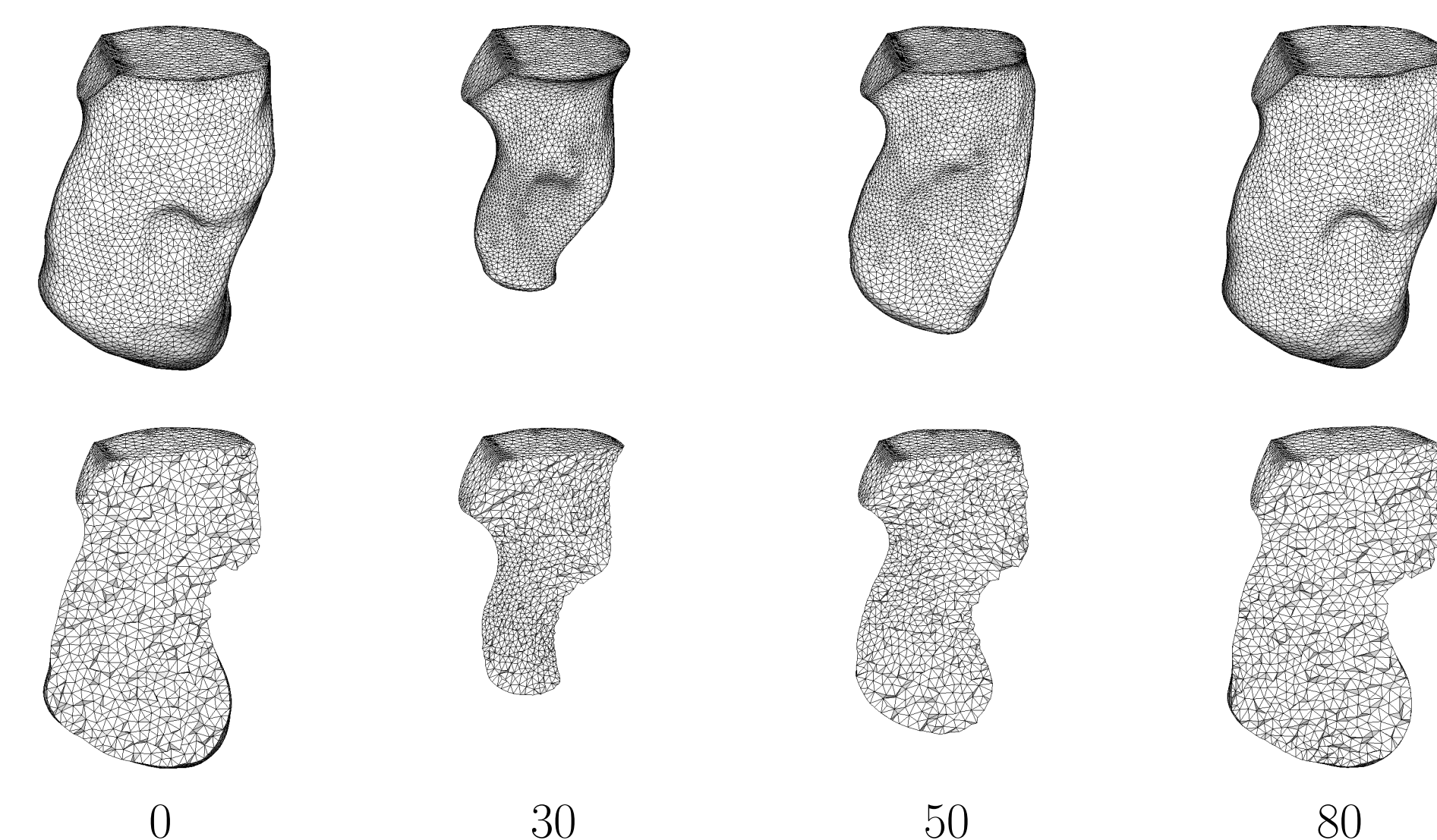


Figure 6: Surface (top row) and volume (bottom row) meshes of the left ventricle for several ceCT images.

Final series of topologically invariant dynamic meshes for the left ventricle based on the dynamic ceCT images contains 14033 nodes and 69257 tetrahedra. Initial ceCT dataset, automatic segmentation, dynamic mesh, and preliminary modeling results are presented in Fig. 5. The flow is modeled by the incompressible Navier–Stokes equations using arbitrary Lagrangian–Eulerian method. Aortic and mitral valves were modeled by switching boundary conditions on the valve planes. For the simplicity of mesh generation and numerical modeling we assumed the position of the valve planes is fixed during the cardiac cycle.

## Adaptive mesh generation

We use several techniques for soft tissue segmentation, including user-guided active contour segmentation with supervised random forest classification and textural features computation [2, 3, 10].

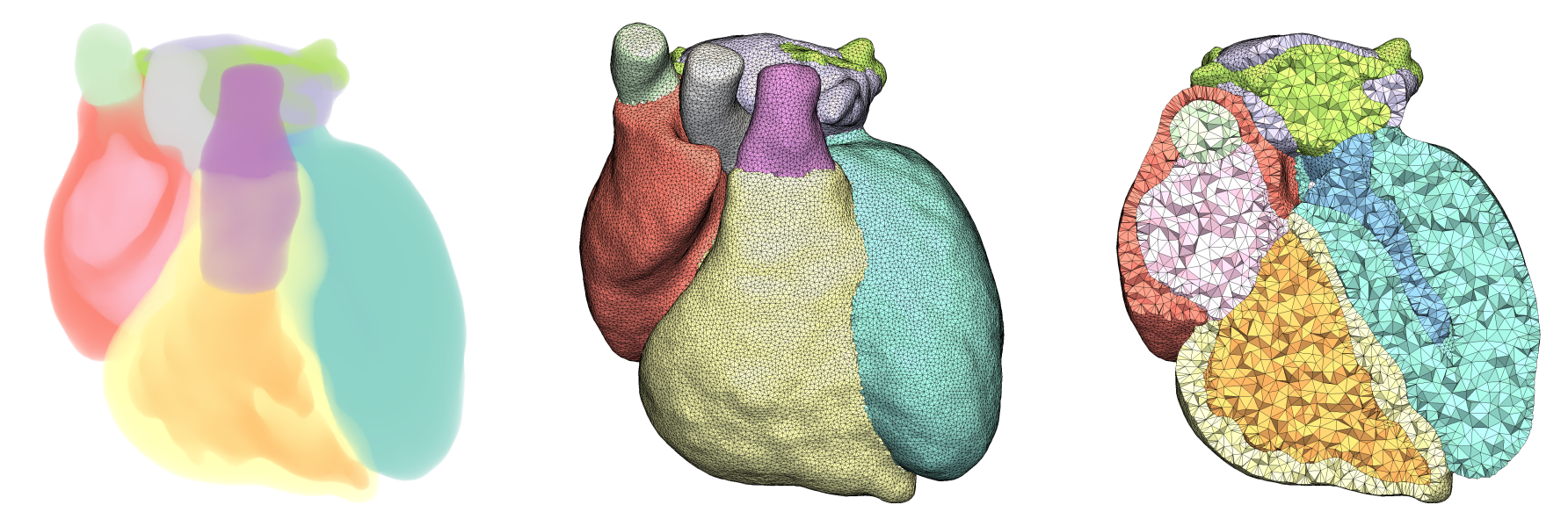


Figure 7: Unstructured mesh for VHP human heart: (left) translucent 3D model, (center) triangular surface mesh, (right) volume cut of the tetrahedral mesh. 367318 tetrahedra and 77953 vertices in the mesh.

Delaunay triangulation algorithm from CGAL Mesh library [11] is used for adaptive unstructured tetrahedral generation. The mesh size in Visible Human Project (VHP) human heart (Fig. 7) is 1–3 mm.

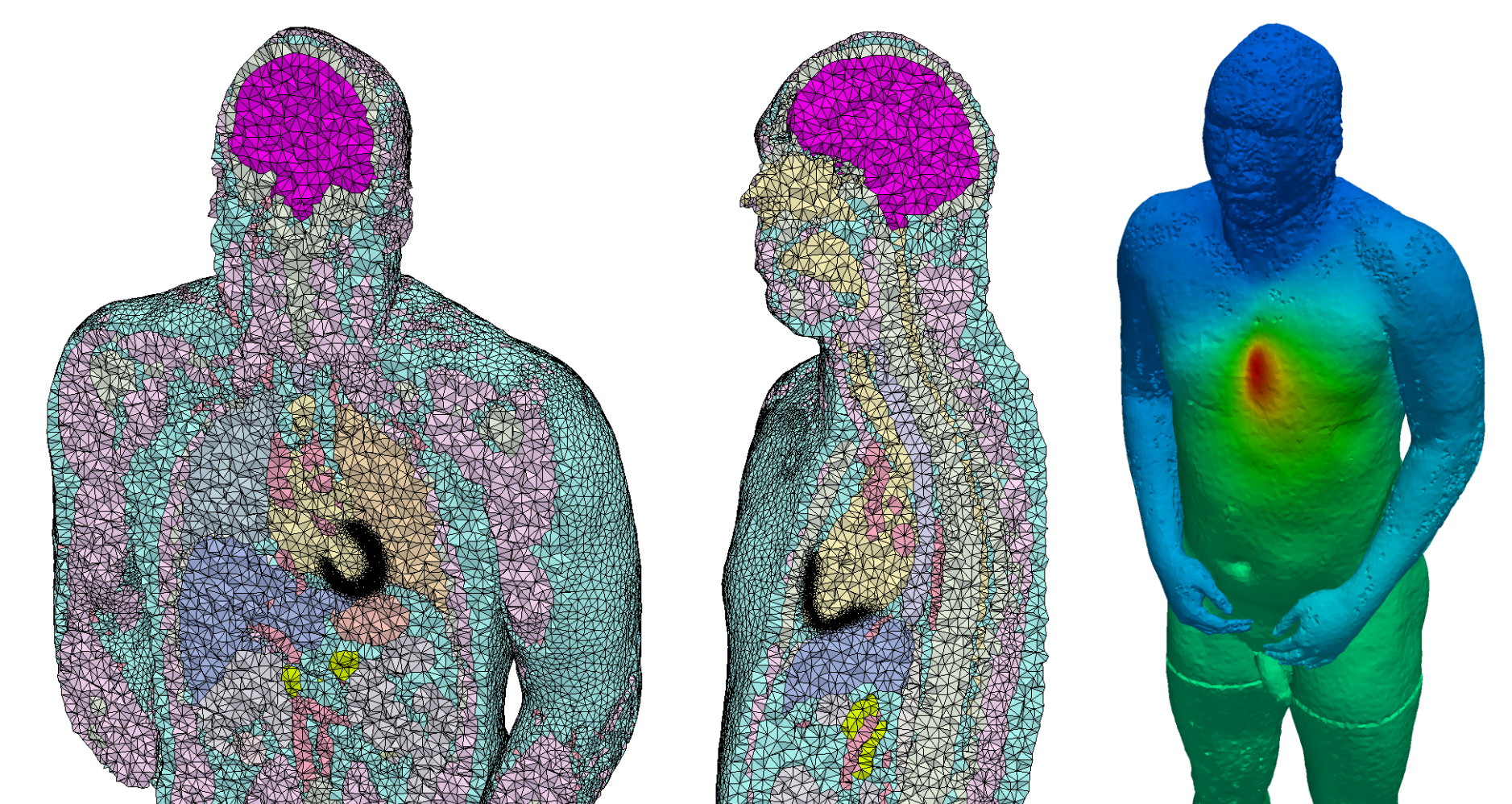


Figure 8: VHP human body mesh refined near heart ventricles (left, center) and surface electrical potential calculated from forward ECG model (right).

We use adaptive mesh to improve mesh resolution in the region of interest while keeping the total number of mesh elements reasonable. Fig. 8 demonstrates the results of forward ECG calculation using adaptive unstructured mesh for full VHP body [10] with 2049945 tetrahedra and 370242 vertices.

## Conclusion

The work addresses several segmentation techniques for generation of individualized computational domains from medical imaging datasets. We propose automatic algorithms for vascular network segmentation. We discuss soft tissue segmentation and adaptive mesh generation. A new technique for segmentation and mesh generation using dynamic ceCT images was proposed. The proposed algorithms are presented in details in our previous works [1, 2, 3, 10].

## Acknowledgments

The authors acknowledge the staff of I. M. Sechenov First Moscow State Medical University and especially Philippe Yu. Kopylov for patient-specific data. The authors thank Alexander V. Lozovskiy for providing preliminary results of left ventricle hemodynamics modeling. The work was supported by the Russian Science Foundation grant 14-31-00024.

## References

- [1] A. Danilov, Y. Ivanov, R. Pryamonosov, and Y. Vassilevski. Methods of graph network reconstruction in personalized medicine. *International Journal for Numerical Methods in Biomedical Engineering*, 32:e02754, 2016.
- [2] A. A. Danilov, R. A. Pryamonosov, and A. S. Yurova. Image segmentation techniques for biomedical modeling: electrophysiology and hemodynamics. In *Proceedings of ECCOMAS 2016*, 2016.
- [3] A. Danilov, R. Pryamonosov, and A. Yurova. Image segmentation for cardiovascular biomedical applications at different scales. *Computation*, 4:35, 2016.
- [4] H. A. F. Gratama van Andel, H. W. Venema, G. J. Streekstra, et al. Removal of bone in CT angiography by multiscale matched mask bone elimination. *Medical Physics*, 34:449–462, 2007.
- [5] L. Grady. Fast, quality, segmentation of large volumes – Isoperimetric distance trees. *Computer Vision – ECCV 2006*, 3953:449–462, 2006.
- [6] A. Frangi, W. Niessen, K. Vincken, and M. Viergever. Multiscale vessel enhancement filtering. In *Medical Image Computing and Computer-Assisted Intervention – MICCAI’98*, 130–137, 1998.
- [7] C. Pudney. Distance-ordered homotopic thinning: A skeletonization algorithm for 3D digital images. *Computer Vision and Image Understanding*, 72:404–413, 1998.
- [8] P. A. Yushkevich, J. Piven, H. C. Hazlett, et al. User-guided 3D active contour segmentation of anatomical structures: Significantly improved efficiency and reliability. *Neuroimage*, 31:1116–1128, 2006.
- [9] J. M. Escobar, E. Rodriguez, R. Montenegro, et al. Simultaneous untangling and smoothing of tetrahedral meshes. *Computer Methods in Applied Mechanics and Engineering*, 192:2775–2787, 2003.
- [10] Y. V. Vassilevski, A. A. Danilov, S. S. Simakov, et al. Patient-specific anatomical models in human physiology. *Russian Journal of Numerical Analysis and Mathematical Modelling*, 30:185–201, 2015.
- [11] L. Rineau, M. Yvinec. A generic software design for Delaunay refinement meshing. *Computational Geometry*, 72:100–110, 2007.

## Contact Information

- Alexander A. Danilov
- e-mail: a.a.danilov@gmail.com

Supplementary materials are available online:  
<http://dodo.inm.ras.ru/danilov/cmb-2017/>

